The Journal of the Astronautical Sciences (2020) 67: 137–163
https://doi.org/10.1007/s40295-019-00187-y

Robust Controller Design of Non-minimum Phase Hypersonic Aircrafts Model based on Quantitative Feedback Theory

Zhaoying Li[1] · **Wenjie Zhou**[1] · **Hao Liu**[1]

Published online: 17 July 2019

Abstract

Hypersonic aircrafts are introduced as a platform for cost-efficient access to space. However, challenging problems of control hypersonic aircrafts exist due to aerodynamic parametric uncertainties, external disturbances and unstable internal dynamics. This paper explores how to design and tune a controller with quantitative feedback theory (QFT). Furthermore, robust controllers based on QFT for longitudinal model are designed to solve the non-minimum phase problem and the large aerodynamic parameters uncertainty problem due to complex flight environment. According to the summary of the plant dynamics and control method, different performance specifications are presented and transformed into a set of design criteria in transfer function form as constrains for the controller design. Simulation results obtained with the designed controller and prefilter demonstrate that the designed robust controller can guarantee the stability of hypersonic aircraft model and satisfy the given performance specifications. Simulation comparisons to LQR control approach are performed to demonstrate the advantages of the proposed QFT robust controller.

Keywords Hypersonic aircrafts · Quantitative feedback theory · Non-minimize phase · Robust control

Introduction

Hypersonic vehicles are introduced as a possible platform for cost-efficient access to near space, as shown in [1]. After the failed test in 2001, NASA tested the scramjet powered X-43A successfully in 2004 and created a world speed record at Mach 9.6 for a jet-powered aircraft, as illustrated in [2]. The feasibility of hypersonic aircrafts was verified in [3] by the scramjet X-43A. Although great substantial progress has

✉ Hao Liu
liuhao13@buaa.edu.cn

[1] School of Astronautics, Beihang University, Beijing, 100191, People's Republic of China

been made recently, the unique dynamics of hypersonic aircrafts poses a challenging problem of control system design that has not been fully studied.

Many challenging problems associate with hypersonic aircrafts, including nonlinear dynamics, uncertainties and strong coupling between aerodynamic and propulsive effects, as described in [4]. Among these difficulties appeared when designing flight control systems for hypersonic aircrafts, one of the largest challenges of the given system for designing robust controllers is the existed unstable zero-dynamics of the non-minimum phase plant system that may appear when ignoring the coupling assumed insignificant to generate the simple model adopted in [5]. In [6–8], robust controllers based on the robust compensating techniques were proposed to restrain the effects of multiple uncertainties for minimum phase systems, but further researches on non-minimum phase systems were ignored. The applications of standard robust control techniques, such as the standard state feedback linearization control strategy and the standard sliding mode control method, on the hypersonic aircrafts involving non-minimum phase behaviors remain challenging.

Several strategies of control system design for hypersonic aircrafts have been adopted to solve the challenging problems. Among these controller design strategies, both linear control and nonlinear control methods are studied. An adaptive mode nonlinear controller was adopted for a generic hypersonic aircraft [9, 10]. A Lyapunov-based exponential tracking control system of a hypersonic aircraft was synthesized in [11]. Fuzzy control strategy was proposed for the hypersonic vehicles in [12] to obtain the robustness properties of the closed-loop control systems. A nonlinear robust controller based on the feedback linearization approach was studied in [13]. In [14], control system based on quasi-continuous high-order sliding mode control method was utilized. Nonlinear robust flight control system based upon disturbance observer was explored in [15]. All of the above controller design methods ignored the non-minimum phase effect existed in hypersonic aircrafts. An output tracking control method was proposed for non-minimum phase flexible air-breathing hypersonic vehicle in [16]. A combination method of the small-gain arguments and the adaptive control techniques was adopted for a hypersonic vehicle model flight control [17]. A neural network augmentation of a linear controller was explored in [18]to deal with the non-minimum phase problem.

In this paper, a robust controller based on the quantitative feedback theory (QFT) method is proposed to solve the non-minimum phase effect. QFT is one of the methods to design robust control systems, which was introduced in [19–21], and has attracted considerable interest over the last three decades. The QFT is a frequency-domain-based design technique and the controllers can be generated to satisfy a set of performance specifications over a given range of plant parameter uncertainty and external disturbance. The QFT technique is based on the classical idea of frequency-domain shaping of the open-loop transfer function, and the QFT concept was extended into nonlinear QFT in order to apply it to nonlinear and linear-time-varying plants, as shown in [20]. Works showed strong underlying connections between the MIMO QFT design methods and other classical multivariable design methods based on dominance theory and sequential loop closure, as illustrated in [22–24]. Despite of thse similarities, the MIMO QFT still stands apart from other classically formulated multivariable design methodologies in its ability to quantitatively treat uncertainty

and enforce frequency domain robust stability and performance specification. Design of robust controllers for uncertain non-minimum phase and unstable plants with the QFT were studied in [25], and the QFT method for solving non-minimum phase system problem was improved in [26].The QFT robust control design technique was adopted for designing of fighter aircrafts pitch rate robust control system, as illustrated in [27]. In [28], the QFT method to design robust longitudinal controllers for unmanned hypersonic vehicles was used. But, the QFT robust controller was mainly designed for minimum phase system, and the problem of robust controller design for non-minimum phase system that may exist in hypersonic vehicles flight was not considered. The aim of this paper is to design robust controller that satisfies the given performance specifications for longitudinal dynamics of hypersonic aircrafts with the QFT technique.

This paper is organized as follows: the QFT robust control design method is described in details in "Quantitative Feedback Theory"; in "Longitudinal Hypersonic Aircraft Model Dynamics", the dynamic model of the hypersonic aircrafts is introduced briefly; the QFT robust control design method of the hypersonic dynamics described by non-minimum phase systems is proposed in "QFT Robust Controller Design"; in "Simulatiom Results", the simulation results are shown and comparison results are presented; conclusions of this paper are drawn in "Conclusions".

Quantitative Feedback Theory

In this section, QFT robust control design philosophy and design procedure are described in details.

Quantitative Feedback Theory

The QFT is an extension of classical frequency robust control design method developed by Horowitz. Generally, the QFT is two degrees of freedom (2-DOF) structure which contains a controller and a prefilter as shown in Fig. 1, whose main objective is to design and implement a 2-DOF robust system for a plant with uncertainty to satisfy the desired performance specifications, while achieving reasonably low loop gains. $R(s)$, $F(s)$, $D(s)$, $G(s)$, $M(s)$, $P(s)$, and $Y(s)$ represent the reference input, designed prefilter, output disturbances, designed robust controller, elevator actuator term, uncertainty plant and output of the system, respectively.

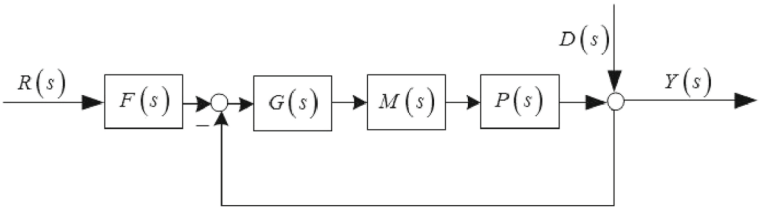

Fig. 1 Canonical 2-DOF feedback structure

Quantitative Feedback Theory Controller Design Procedure

The robust controller design with QFT method contains several specific steps:

1. Plant model and templates generation
   The plant dynamic models are described by a set of linear invariant (LIT) transfer function with uncertainty over the desired operating frequency range. The plant uncertainties contain both structured uncertainty which implies variation in plant parameters and unstructured uncertainty. Taken the plant parameter uncertainty into account, the process of every frequency of interest generalizes the plant uncertainty templates which are sets of complex numbers representing the frequency response of the group of uncertain plants at a fixed frequency. The uncertainty of the plant is described by templates on Nichols chart, representing the gain and phase variation at each chosen frequency of the system frequency response over the operating range. Techniques adopted to compute the templates were studied in [29].
2. Frequency array selection
   Prior to design the QFT robust controller and prefilter, a frequency array at which various performance specification function bounds and the templates are computed must be taken into account. Since the selection of frequency array needs some engineer experience, the experienced engineers can often tell the frequencies of interest. Strict criterion adopted to choose the frequency array is not stated. In order to guarantee the robustness of the designed QFT controller, frequencies at which the templates have large uncertainties should be selected as part of the frequency array. This can be obtained from the BODE chart of the set of plants with uncertainties.
3. Performance specifications design
   The selection of performance specifications contains the steady-state and the dynamic performance of the closed-loop plant. The performance specifications often contain robust specification, reference tracking specification, sensor noise attenuation and disturbance rejection which can be given in terms of gain and phase margin or equivalent transfer functions. The performance specifications can be defined either in time domain or in frequency domain. In the time domain, performance specifications are often represented by settling time t_s, rise time t_r, maximum peak overshoot M_p. However, all of the performance specifications given in time domain should be transformed into the frequency domain so that corresponding boundaries can be generalized in the Nichols chart. Suitable frequency domain transfer function performance specifications can be normally possible to find and should be equipped with the character of simplicity and meet the specifications. Generally, a second-order transfer function with different damp ratio and natural frequency can be chosen and synthesized. Then poles and zeros can be added to the transfer function to meet the specifications more closely.
4. Nominal plant selection
   The uncertainty set of system plant cannot be used directly to design QFT robust controller. One nominal transfer function should be selected from the

uncertainty set as a standard used in the following QFT robust controller design and prefilter synthesis.

5. QFT bounds generation

   Performance specifications synthesized and templates generated above are used to produce bounds at the selected frequencies in the frequency domain. The robust stability specification, disturbance rejection specification and reference specification generate corresponding bounds on Nichols chart. Once these bounds have been computed, the worst case bound or the restrictive bound can be calculated at the selected frequency array and integrated together to generate an intersection bound which is used for controller design in the following loop shaping stage (see e.g., [30–33]).

6. Loop shaping and the QFT controller design

   The QFT controller design is performed on the Nichols chart by adding gains, poles and zeros. This is a loop-shaping process of open-loop nominal plant transfer function

$$L_0(s) = G(s) M(s) P_0(s), \tag{1}$$

   The result of the loop-shaping of nominal plant transfer function $L_0(j\omega)$ must guarantee that the transfer function with synthesized controller must lie on or above the bounds at each of the selected frequencies.

   One of the advantages of utilizing loop-shaping method to design the QFT controller on the Nichols chart is that the process of controller design is transparent and compensation can be improved gradually so that the adjustment of the controller are explicit at each step. This design method can make a proper trade-off between the performance specifications and the complexity of the controller transparently.

7. Prefilter design

   The designed QFT controller by loop-shaping on the Nichols chart ensures the robust stability and disturbance rejection specification of the closed loop transfer function frequency response. However, in order to guarantee the plant satisfies certain tracking specification, a prefilter must be designed to shape the output of the system. This process is also performed on the frequency domain, and Bode diagram is adopted. The reference tracking specifications are transformed into the specification envelope on the Bode diagram and the prefilter is synthesized to shift the frequency response of the closed-loop system into the formed tracking specification envelope.

8. Analysis and design validation

   The QFT controller is synthesized at the trail selected frequency array, but the frequency response of the closed-loop system with designed controller should necessarily be analyzed at all the frequencies instead of just the selected ones to guarantee that the designed controller satisfies all the specifications at all the frequencies. In this part, both frequency domain response and time domain response of the plant with the designed QFT controller and prefilter are available to check the final performance . The analysis of the finished QFT controller and prefilter may demonstrate that performance specifications at some frequencies are not completely met due to the omitting of some frequencies at the frequency array

selection step. Once these cases appear, iterations could be carried out to select new frequency array to guarantee the ignored frequencies taken into account and all the bounds computed.

Longitudinal Hypersonic Aircraft Model Dynamics

The hypersonic aircraft model considered in this paper is presented in [34]. And this model was also used in [28] where a QFT robust controller has been designed for minimum phase. Assuming the coupling terms sideslip angle β , yaw angle rate r , roll angle μ and roll angle rate p are zeros, then the longitudinal hypersonic aircraft dynamic model can be described by Lagrange's equations as follows:

$$\begin{aligned} \dot{\alpha} &= \frac{1}{mV}(-L + mg\cos\gamma) + q, \\ \dot{q} &= \frac{M}{I_{yy}}, \end{aligned} \tag{2}$$

where V, γ, α, q, m, g, and I_{yy} are the velocity, flight path angle, attack angle, the pitch rate, mass, gravitational constant, and moment of inertia, respectively. L and M represent the lift force and pitching moment, and satisfy that

$$\begin{aligned} L &= \frac{1}{2}\rho V^2 S C_\alpha, \\ M &= \frac{1}{2}\rho V^2 S c_A C_{M\alpha}, \end{aligned} \tag{3}$$

where ρ, c_A, S, C_α, and $C_{M\alpha}$ represent the air density, mean aerodynamic chord, reference area, lift force aerodynamic coefficient and pitching moment aerodynamic coefficient, respectively.

$$\begin{aligned} C_\alpha &= \bar{C}_\alpha + \Delta C_\alpha, \\ C_{M\alpha} &= \bar{C}_{M\alpha} + \Delta C_{M\alpha}, \end{aligned} \tag{4}$$

where $\bar{C}_\alpha$ and $\bar{C}_{M\alpha}$ indicate the nominal part of the aerodynamic coefficient while $\Delta\bar{C}_\alpha$ and $\Delta\bar{C}_{M\alpha}$ represent the uncertainty part of the aerodynamic coefficient. In this paper, 20% uncertainty of nominal aerodynamic coefficients is considered. The decoupled longitudinal hypersonic aircraft plant is linearized with the small perturbation linearization method. The linearized dynamic model is presented in next section and the transformation of the longitudinal hypersonic aircraft model from state space form to transfer function form is described.

Longitudinal Hypersonic Aircraft Model Dynamics

Linearized uncertainty dynamic model of hypersonic aircraft is required to design QFT robust controller for guaranteeing longitudinal stability. The elevator actuator

Table 1 Longitudinal system coefficients

Parameter	Values	Parameter	Values
a_{11}	−0.183	a_{22}	0
a_{12}	1	b_1	−0.0042
a_{21}	0.0786	b_2	−0.0041

dynamics must be considered and the elevator actuator for hypersonic aircrafts can be described by the following first-order transfer function:

$$\frac{\delta_e(s)}{\delta_{e_c}(s)} = \frac{100}{s+100}, \tag{5}$$

where δ_{e_c} indicates the elevator deflection command and δ_e represents the real the elevator deflection. The small perturbation linearization method is adopted in this paper to linearize the longitudinal model of the hypersonic aircraft. After linearization, the linearized longitudinal hypersonic aircraft model can be presented by the following canonical linear time-invariant state space equation:

$$\begin{aligned} \dot{x} &= Ax + Bu, \\ y &= Cx. \end{aligned} \tag{6}$$

The state vector and outputs of the longitudinal system are chosen as $x = \left[\, \alpha \;\; q \,\right]^T$, $y = \left[\, \alpha \;\; q \,\right]^T$.

The input of the longitudinal system is given by:

$$u = \delta_e. \tag{7}$$

The longitudinal system matrices are shown below:

$$A = \begin{bmatrix} a_{11} & a_{12} \\ a_{21} & a_{22} \end{bmatrix}, B = \begin{bmatrix} b_1 \\ b_2 \end{bmatrix}, C = \begin{bmatrix} 1 & 0 \\ 0 & 1 \end{bmatrix}, \tag{8}$$

where the variables $a_{ij}, b_i\ (i, j = 1, 2)$ represent the linearized system dynamic coefficients and can be obtained from Table 1.

Remark 1 The hypersonic aircraft system was originally modeled as a state space form as shown in Eq. 8, however, the QFT robust control design is based on transfer function. Then the state space form of the hypersonic aircraft model must be transformed to transfer function form. Thus, before design the QFT robust controller, the transfer function form of the hypersonic aircraft system should be obtained.

Pitch Attitude Control System Model

The transformed transfer function form is shown as follow:

$$\frac{q}{\delta_e} = \frac{k_0(s+z_0)}{(s+p_{01})(s+p_{02})}, \tag{9}$$

Table 2 Longitudinal open-loop transfter function coefficients

State number	1	2	3	4	5
Mach number	4.38	4.00	3.39	2.99	2.37
k_0	0.00116	0.00079	0.00199	0.00266	0.00406
z_0	0.04754	0.03266	0.09007	0.13080	0.26360
p_{01}	0.16210	0.12960	0.21770	0.26070	0.38640
p_{02}	-0.1266	-0.1057	-0.1537	-0.1694	-0.2034

where the parameters k_o, z_o, p_{o1}, and p_{o2} represent the gain, zero and poles of the open-loop transfer function from pitch rudder defection to pitch angle rate and the parameters can be obtained from Table 2. Five states of different Mach number are shown in Table 2.

The longitudinal control system is shown in Fig. 2. In the system, $F(s)$, $D(s)$, $G_1(s)$, $G_2(s)$, $M(s)$, and $P(s)$ represent the designed prefilter, external disturbances, synthesized outer-loop robust controller, inner-loop robust controller, elevator actuator term and uncertainty plant of pitch angle system, respectively. θ_c is the given pitch angle command, q and θ are real pitch angle rate and real pitch angle.

A two-loop QFT robust control strategy is adopted to design QFT robust controller and prefilter and the control law below is utilized:

$$\delta_e = G_2(s)\left(G_1(s)\left(F(s)\theta_c - \theta\right) - q\right). \tag{10}$$

QFT Robust Controller Design

The QFT robust controller design method and procedure have been presented previously, then controller design will be performed following the previous procedure in this section step by step. First, the method of performance specification selection is introduced. Then, criterions for choosing frequency array are described and the completed QFT robust controller design process of inner-loop and outer-loop is presented in this section.

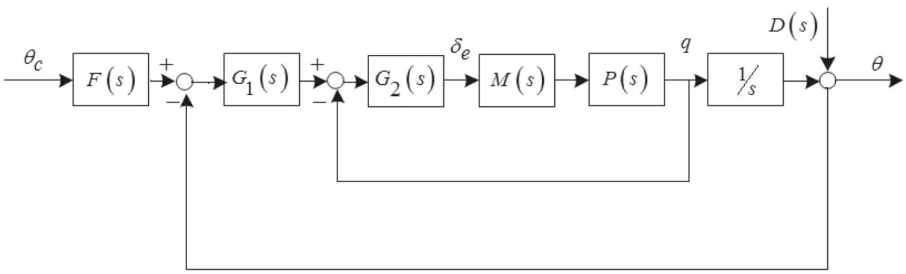

Fig. 2 Longitudinal pitch attitude control system

Table 3 Design inner-loop controller coefficients

Parameter	Values
Overshoot	$M_p \leq 10\%$
Rise time	$t_r \leq 0.25s$
Settling time	$t_s \leq 0.25s$

Performance Specifications Selection

The hypersonic aircraft control system should be with the ability of guaranteeing stability, disturbance rejection and reference signal tracking specifications to deal with the wide dynamic range uncertainty of aerodynamic coefficients which caused by large Mach-Altitude flight environment and aerodynamic coefficients uncertainties.

Tracking Performance Specification

The tracking performance specification is provided for guaranteeing that the uncertainty hypersonic vehicle system which is caused by aerodynamic uncertainties and external disturbance has the acceptable range of closed-loop tracking response. Tracking specifications are generally given in the time domain as settling time t_s, rise time t_r, and maximum peak overshoot M_p, which can then be transformed into the frequency domain as:

$$T_{TL}(j\omega) \leq T_T(j\omega) \leq T_{TU}(j\omega), \tag{11}$$

where $T_{TL}(j\omega)$, $T_T(j\omega)$, and $T_{TU}(j\omega)$ describe the transfer function of lower bound, closed-loop transfer function and upper bound transfer function, respectively.

For the longitudinal hypersonic vehicle system, the time domain pitch angle tracking specifications are given in Table 3.

The upper tracking bound transfer function model is determined by the time domain specifications settling time t_s, rise time t_r, and maximum peak overshoot M_p, and the lower bound transfer function which is always without overshoot is determined by settling time t_s and rise time t_r. The upper bound tracking function is first defined by a second-order model:

$$T_{TU}(s) = \frac{\omega_n^2}{s^2 + 2\zeta\omega_n + \omega_n^2}, \tag{12}$$

where ω_n indicates the natural frequency and ζ represents the damp ratio.

For second-order system $T_{TU}(s)$, one can obtain that :

$$\begin{aligned} M_p &= e^{-\frac{\pi\zeta}{\sqrt{1-\zeta^2}}}, \\ t_r &= \frac{1}{\omega_n\sqrt{1-\zeta^2}}\left[\pi - \tan^{-1}\frac{\sqrt{1-\zeta^2}}{\zeta}\right], \\ t_{s[5\%]} &\approx \frac{3}{\zeta\omega_n}. \end{aligned} \tag{13}$$

According to the given time-domain performance specification settling time t_s, rise time t_r, and overshoot M_p, natural frequency ω_n and damp ratio ζ can be approximately computed as 0.65 and 15. In order to adjust the upper tracking bound transfer function in the high frequency range, one zero is considered and the selected upper tracking bound transfer function is shown below:

$$T_{TU} = \frac{225\,(0.02s+1)}{s^2+19.5s+225}. \tag{14}$$

The method of choosing lower tracking bound transfer function is the same as the upper tracking bound. However the lower tracking bound has no overshoot and is represented by the following expression:

$$T_{TL} = \frac{1629}{s^3+29s^2+361s+1629}. \tag{15}$$

Robust Stability Performance Specification

The required performance specifications are phase margin of 45^o and magnitude margin of 5 dB and the stability performance specification can be represented by the following expression:

$$\left|\frac{L(j\omega)}{1+L(j\omega)}\right| \le \mu = 1.25dB, \tag{16}$$

where $L(j\omega)$ defines the open-loop transfer function of the longitudinal hypersonic vehicle model. This specification can be transformed into frequency domain and described by phase margin and magnitude margin as follows:

$$\begin{aligned} h_p &= 20\lg\left(1+\frac{1}{\mu}\right) = 20\lg(1.9) = 5.1055 > 5dB, \\ \gamma &= 180^\circ - \cos^{-1}\left(\frac{1}{2\mu^2}-1\right)\frac{180^\circ}{\pi} = 47.089^\circ > 45^\circ, \end{aligned} \tag{17}$$

which describes that the selected robust stability performance specification satisfies the desired specification.

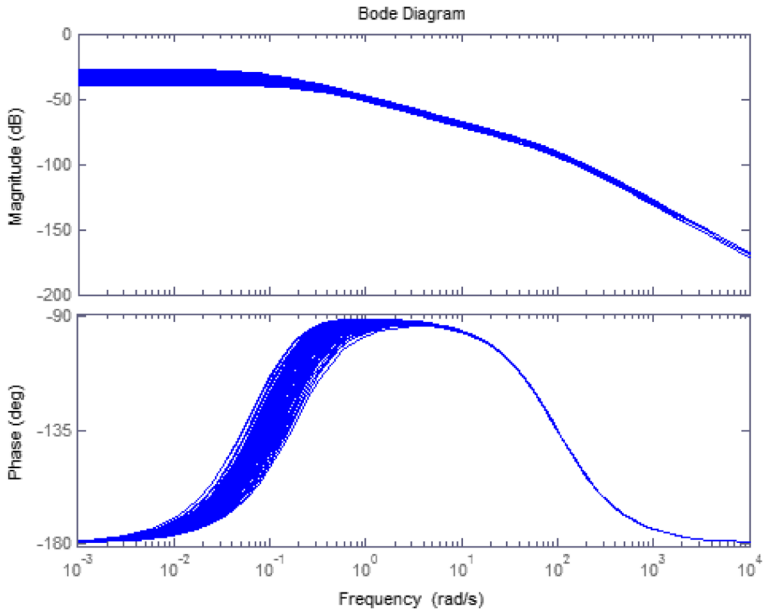

Fig. 3 Bode diagram of uncertainty plant set

Output Rejection Performance Specification

In order to ensure the designed QFT robust control system can provide longitudinal hypersonic vehicle with the ability of rejecting external disturbance, corresponding output disturbance specification is chosen as follow:

$$T_{Ru} = \frac{s^2 + 60s}{s^3 + 120s^2 + 2000s + 1629}, \tag{18}$$

which can reject the step external output disturbance signal into 0.5% of the disturbance signal at $0.5s$.

Frequency Array Selected

A set of plants contain of uncertainty is obtained, from the Bode diagram of the set of uncertainty plants, one can get that in the frequency of $\omega_t = \{0.001, 0.05, 0.1, 0.5, 1, 5, 10, 50100\}$ the magnitude and phase of the plants have large uncertainty range as shown in Fig. 3. Therefore, the frequency is initially selected as $\omega_t = \{0.001, 0.05, 0.1, 0.5, 1, 5, 10, 50100\}$.

QFT Robust Controller Design

The QFT controller and prefilter design are carried out on Nichols Chart and based on classical loop-shaping theory. The objective is to trade-off between the desired performance specifications and complexity of the synthesized QFT robust controller.

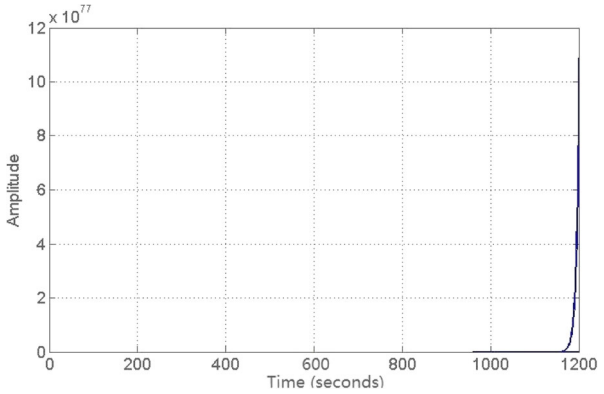

Fig. 4 Step response of pitch attitude model without control

The QFT robust controller should be synthesized to guarantee that the low-frequency bounds troughs should be passed through by the open-loop frequency response.

Inner-loop Controller Design

As can be seen from Table 1, right half plane poles are existed in longitudinal hypersonic aircraft model. Therefore, traditional QFT method for designing minimum phase system robust controller is not satisfied. Then approach for dealing with non-minimum phase system robust controller design problem has been introduced in [25] and improved in [26].

The SISO non-minimum phase uncertain plant can be written in the form as shown in Eq. 19:

$$T(s) = \frac{z(s)\,\widehat{z}(-s)}{p(s)}, \tag{19}$$

where $p(s)$, $\widehat{z}(-s)$, and $z(s)$ represent the left half-plane zeros, right half-plane zeros and left half-plane poles, respectively.

A nominal plant with the plant is chosen and shown by

$$T_0(s) = \frac{z_0(s)\,\widehat{z}_0(-s)}{p_0(s)}. \tag{20}$$

A new nominal plant can be defined as

$$T_0{}'(s) = T_0(s)\,A^{-1}(s) = \frac{z_0(s)\,\widehat{z}_0(s)}{p_0(s)}, \tag{21}$$

if $A(s) = \widehat{z}_0(-s)/\widehat{z}_0(s)$. It can be noted that $T_0{}'(s)$ is a stable minimum phase plant. Then the bounds of robust stability, tracking and disturbance rejection specifications computed on the Nichols chart for $T_0{}'(j\omega_i)$ are the same as that for $T_0(j\omega_i)$ with a horizontal shift of phase $-\arg(A(j\omega_i))$ at selected frequency ω_i [29–31].

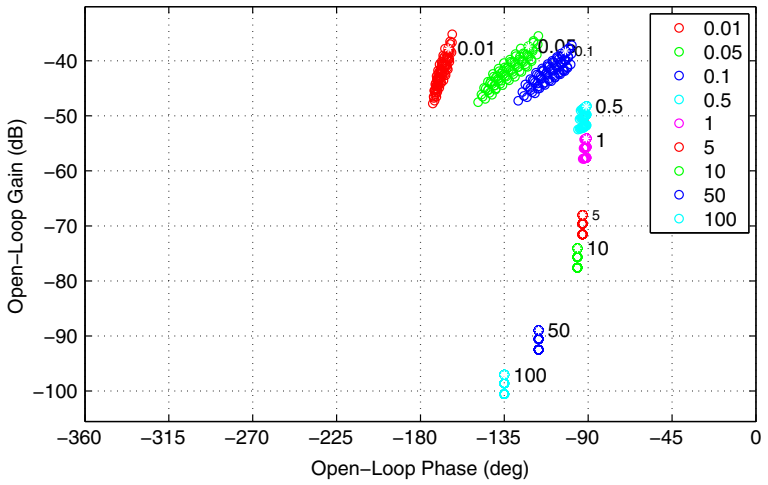

Fig. 5 Plant frequency response templates of inner-loop

As can be seen in Fig. 4, it indicates the step response of pitch angle of uncertainty longitudinal hypersonic aircraft, which demonstrates that the pitch angle system is unstable.

The object of inner-loop QFT robust controller design is to guarantee that the longitudinal hypersonic aircraft plant can be stable with the synthesized the QFT robust controller. Therefore, only robust stability specification is needed in inner-loop QFT controller design. The given robust stability specification is shown in Eq. 16. The templates of the plant which contains aerodynamic parameter uncertainty preformed on the Nichols chart present the variation of open loop gain and phase at the selected frequency points are computed in the Nichols chart as illustrated in Fig. 5. One of the templates is chosen as the nominal plant and the state 4 in Table 1 is selected as nominal plant used to design QFT controller. Figure 6 shows the stability specification which contains magnitude and phase bounds in Nichols chart at each selected frequency points. The robust stability specification bounds and open-loop plant transfer function are plotted in Fig. 7.

Remark 2 As can be seen in Fig. 6, the bounds for the new nominal plant $T_0'(j\omega_i)$ at different frequencies are obtained by shifting the bounds for the nominal plant $T_0(j\omega_i)$ by $-\arg(A(j\omega_i))$. It should be noted that the bounds shifting are not significant, which demonstrates that $-\arg(A(j\omega_i))$ is not large. From $A(s) = \widehat{z}_0(-s)/\widehat{z}_0(s)$, it can be obtained that the bounds shifting would be significant if the unstable zero is large.

Two controllers are designed for the inner-loop and the different loop-shaping results of the open-loop transfer function are plotted in Figs. 8 and 9, respectively. As can be seen, frequency responses of open-loop plant after loop-shaping don't intersect with the robust stability bounds, which demonstrates that both designed

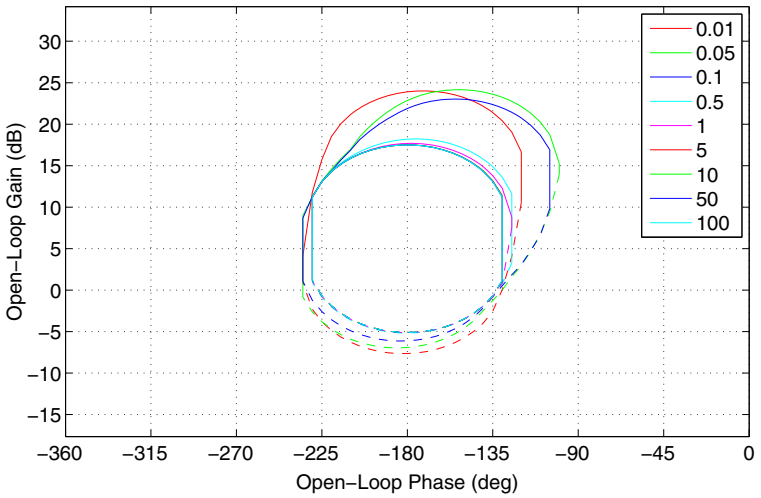

Fig. 6 Robust stability margin bounds of inner-loop

controllers satisfy the desired design requirements. Further results are tested in time domain and step responses of closed-loop transfer function with two different are presented in Figs. 10 and 11.

The designed QFT robust controllers of the inner-loop system are shown as follows:

$$K_1(s) = \frac{k_{in1}(s/z+1)}{(s/p+1)}, \tag{22}$$

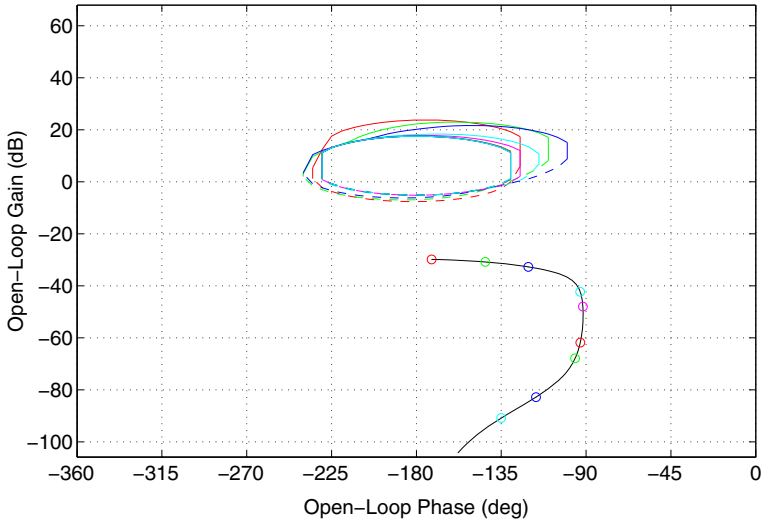

Fig. 7 Robust stability margin bounds without controller of inner-loop

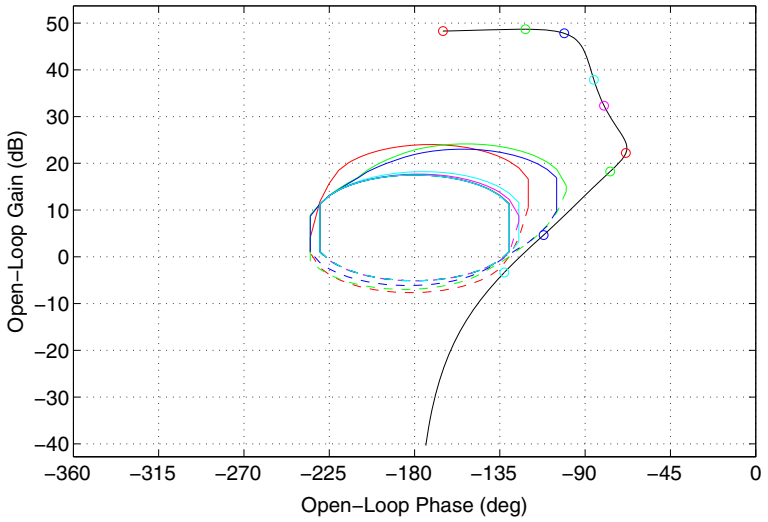

Fig. 8 Open-loop frequency response with controller K_1 of inner-loop

$$K_2(s) = k_{in2}. \tag{23}$$

The coefficients of the designed inner-loop QFT robust controller can be obtained in Table 4.

As can be seen from Figs. 10 and 11, both controllers can stabilize the non-minimum phase plant and the control effects are basically the same. Thus due to the design trade-offs between specifications satisfaction and controller complexity

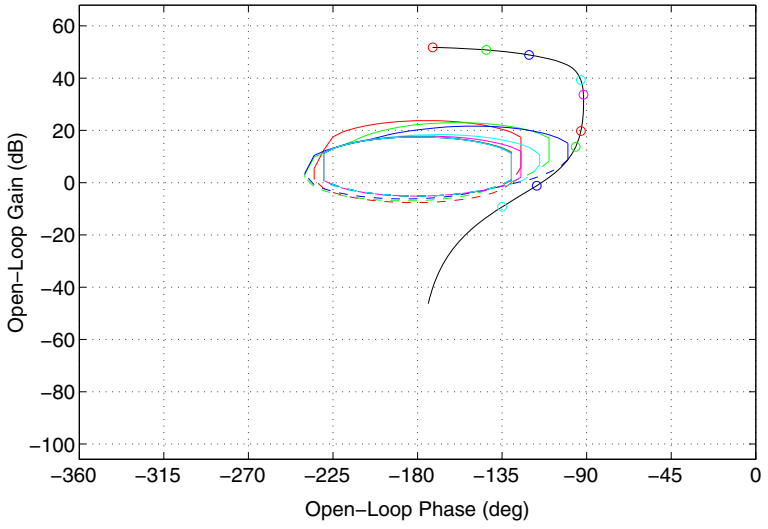

Fig. 9 Open-loop frequency response with controller K_2 of inner-loop

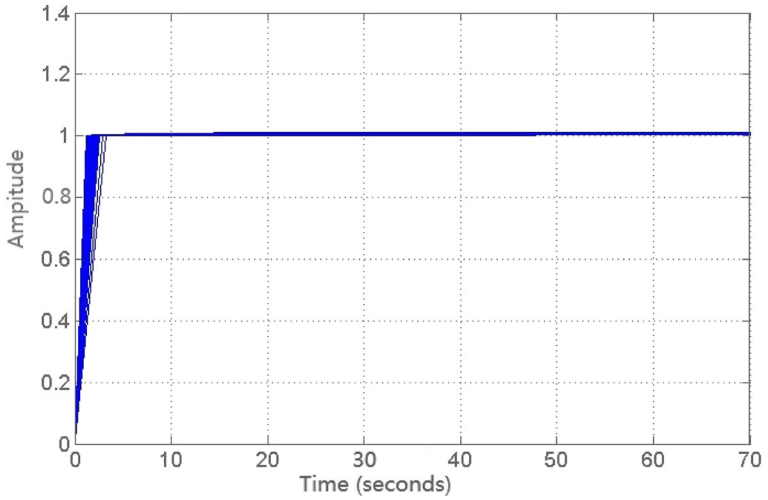

Fig. 10 Closed-loop step response with controller K_1 of inner-loop

principle, then the simpler controller is chosen as the inner-loop controller and the inner-loop controller is

$$G_2(s) = K_2(s). \tag{24}$$

The robust stability specification is illustrated in Fig. 12, in which the solid line represents the closed-loop transfer function of longitudinal hypersonic aircraft system with the designed controller and prefilter while the dashed line indicates the desired robust stability specification. It significantly shown that the solid line is under

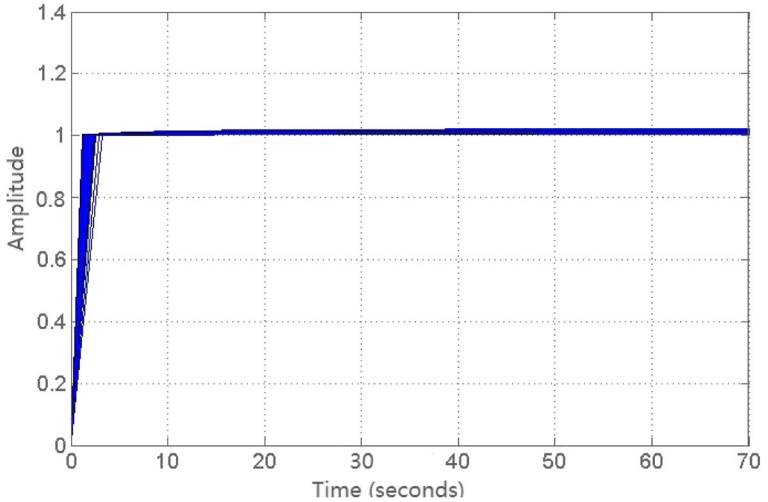

Fig. 11 Closed-loop step response with controller K_2 of inner-loop

Table 4 Designed inner-loop controller coefficients

Parameter	Values	Parameter	Values
k_{in1}	20000	p	9.4894
k_{in2}	12000	z	2.9615

the dashed line, which demonstrates the designed controller and prefilter satisfy the given robust stability specification.

The non-minimum problem exist in the longitudinal hypersonic aircraft plant can be significantly settled with the designed inner-loop controller $G_2(s)$, and the step response of the pitch angle rate as shown in Fig. 11 demonstrates the synthesized QFT robust controller of the inner-loop can stabilize the plant rapidly. Simultaneously, the inner-loop QFT robust controller causes a considerable reduction in uncertainty, which can reduce in outer-loop uncertainty and facilitate the design of outer-loop QFT robust controller.

Outer-loop Controller Design

The templates of the plant which contains aerodynamic parameter uncertainty preformed on the Nichols chart present the variation of open loop gain and phase at the selected frequency points are computed in the Nichols chart as illustrated in Fig. 13. One of the templates is chosen as the nominal plant and the state 4 in Table 1 is selected as nominal plant used to design QFT controller and prefilter. Fig. 14 shows the stability specification which contains magnitude and phase bounds in Nichols chart at each selected frequency points. This also specifies the disturbance bound on the Nichols chart as shown in Fig. 15.

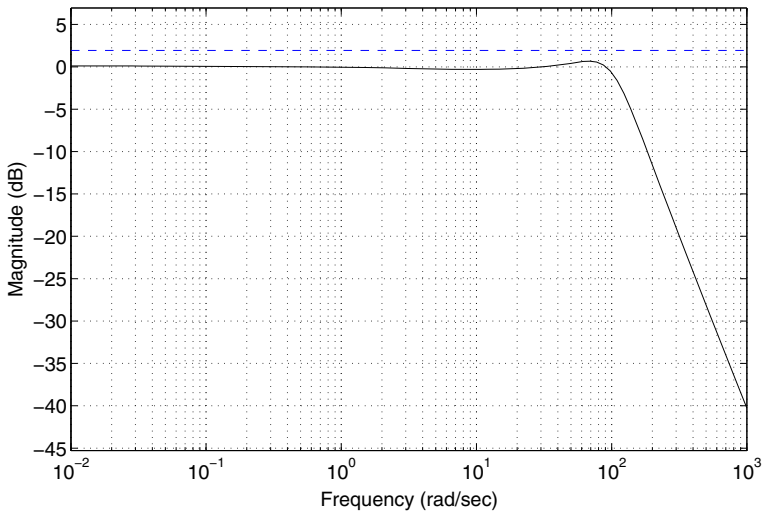

Fig. 12 Analysis of robust stability margin in frequency domain

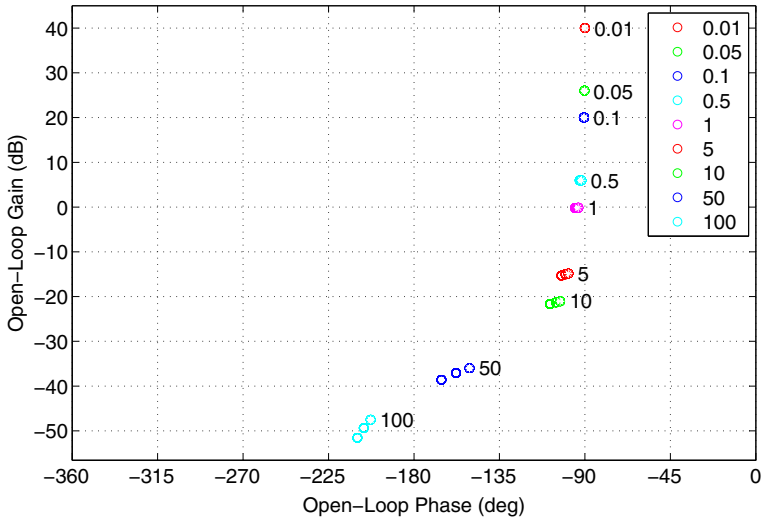

Fig. 13 Plant frequency response templates of outer-loop

Similarly, Fig. 16 presents the tracking performance specification bounds on Nichols chart.

The composite bounds of all the above performance specification and open loop plant template plotted on Nichols chart described in Fig. 17 are adopted to synthesize the desired loop transfer function. The objective is to ensure the magnitude of the open-loop transfer function at each selected frequency above the composite bounds at corresponding frequency points by loop-shaping the open-loop transfer function

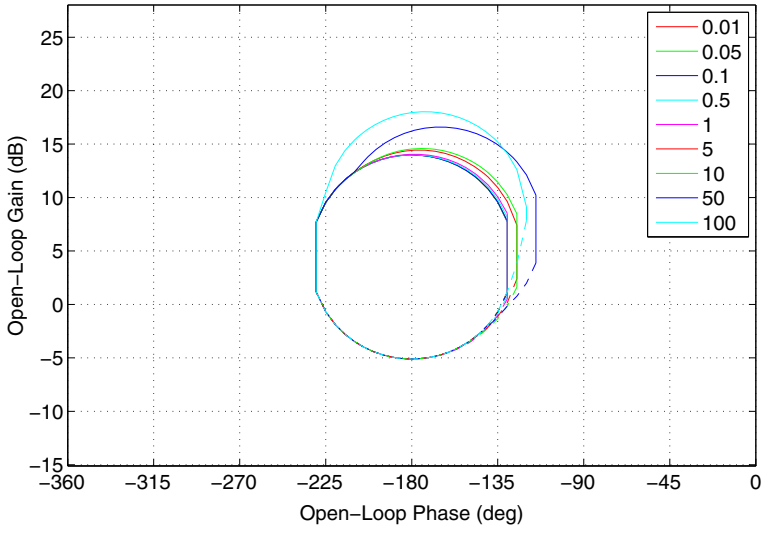

Fig. 14 Robust stability margin bounds of outer-loop

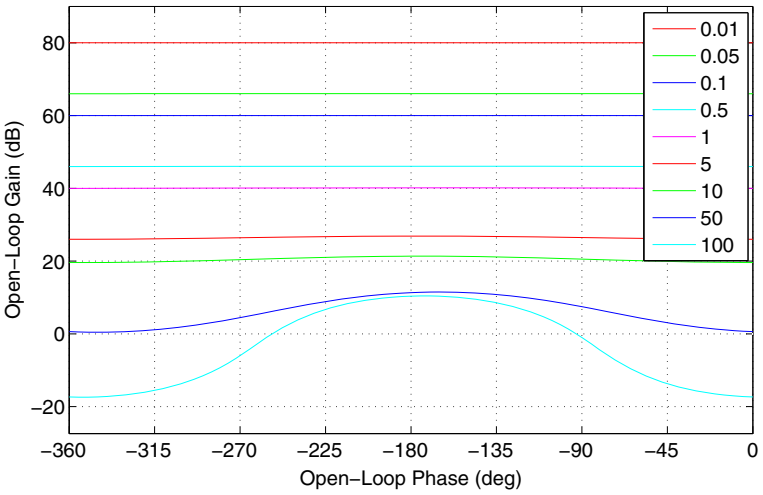

Fig. 15 Robust output disturbance rejection bounds of outer-loop

with selected proper zeros, real and complex poles which synthesize the robust QFT controller.

The result of loop-shaping is plotted in Fig. 18 which indicates that the elements of the controller that added to the nominal plant are satisfied to the composite performance specification bounds.

Figure 19 demonstrates the result of the designed prefilter on the basis of designed controller. The designed controller only guarantees the system closed loop transfer function bound at each selected frequency points on Nichols chart is equal to

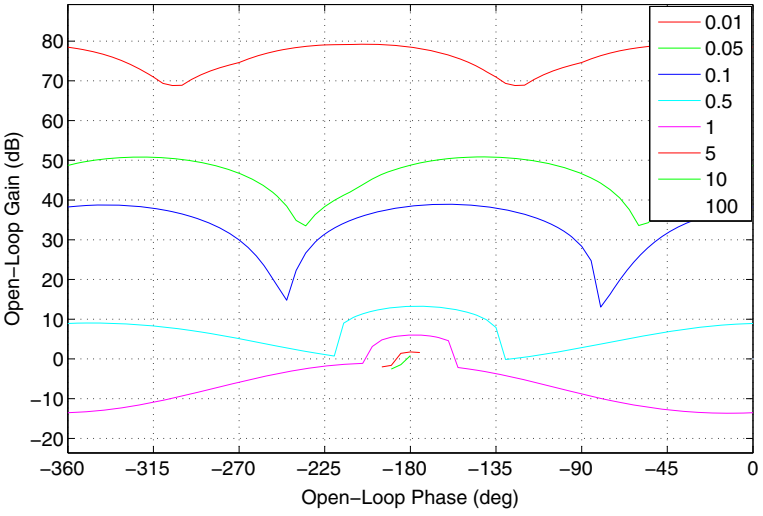

Fig. 16 Robust tracking bounds of outer-loop

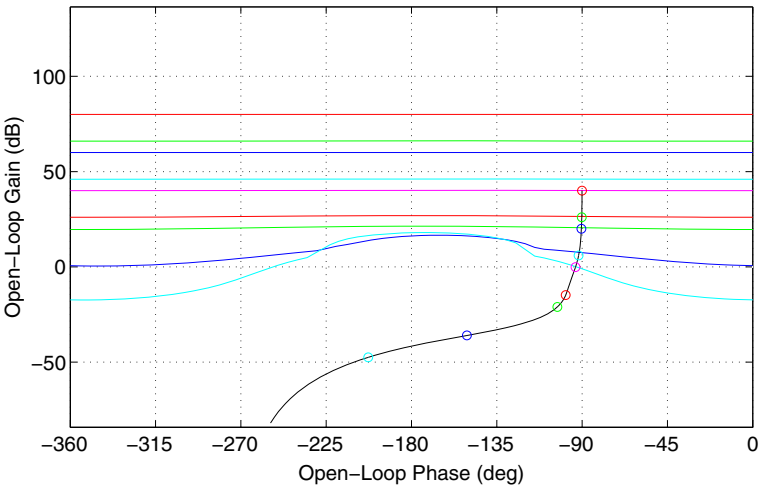

Fig. 17 Open-loop frequency response without controller of outer-loop

or greater than the permissible bound. It could not guarantee the closed-loop transfer function envelope in the performance specifications envelope. Hence a prefilter should be designed to adjust the closed-loop transfer function envelope of the system inside the specifications envelope.

The designed outer-loop QFT robust controller and prefiler are shown below and the corresponding coefficients are indicated in Tables 5 and 6.

Outer-loop controller:

$$G_1(s) = \frac{k_{out}\,(s/z_1+1)\,(s/z_2+1)\,(s/z_3+1)}{(s/p_1+1)\left(s^2/\omega^2+2\xi s/\omega+1\right)}. \tag{25}$$

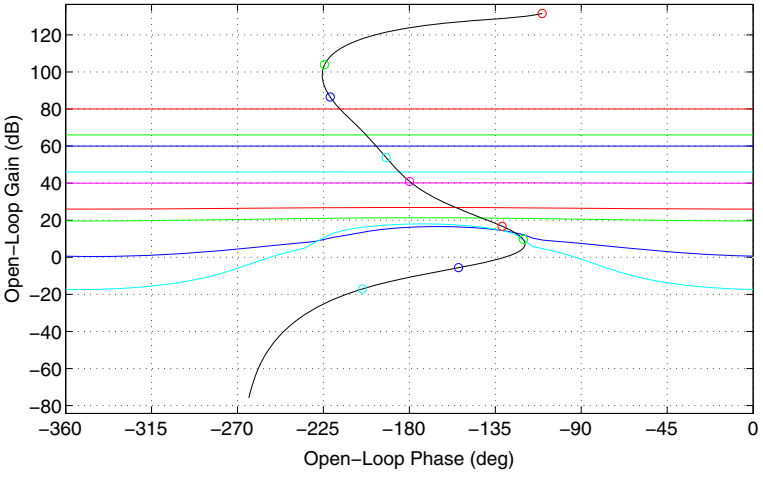

Fig. 18 Open-loop frequency response with controller of outer-loop

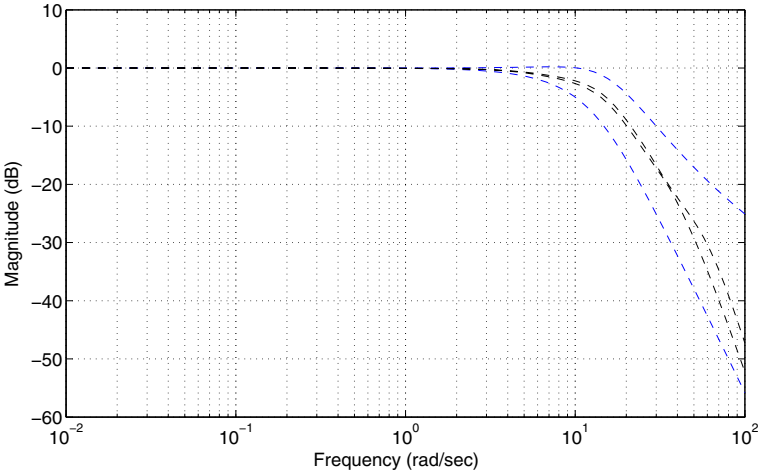

Fig. 19 Closed-loop frequency response with prefilter

Prefilter:

$$F(s) = \frac{\left(s/z_{f1} + 1\right)\left(s/z_{f2} + 1\right)}{\left(s/p_{f1} + 1\right)\left(s^2/\omega_f^2 + 2\xi_f s/\omega_f + 1\right)}. \tag{26}$$

Simulatiom Results

Since the synthesized QFT robust controller and prefilter are designed at limited selected frequency array, validation of the controller and prefilter should be taken into account at all frequencies. Therefore, the next step is to validate the performance of the controller and prefilter. If the validation is failed, frequencies at which the system plant has large uncertainty may not be considered, which demonstrates new frequency array should be selected again and the QFT controller should be redesigned with the same design process below.

The frequency domain robust stability specification is illustrated in Fig. 20, in which the solid line represents the closed-loop transfer function of longitudinal hypersonic aircraft system with the designed controller and prefilter while the dashed line indicates the desired robust stability specification. It significantly shown that the

Table 5 Design outer-loop controller coeffocients

Parameter	Values	Parameter	Values
k_{out}	32842.1	z_1	0.1872
p_1	0.83928	z_2	2.5276
ξ	0.40960	z_3	1.2707
ω	0.02216		

Table 6 Designed prefilter coefficients

Parameter	Values	Parameter	Values
p_{f1}	5.05728	z_{f1}	10.7666
ξ_f	0.58568	z_{f2}	9.4569
ω_f	10.1303		

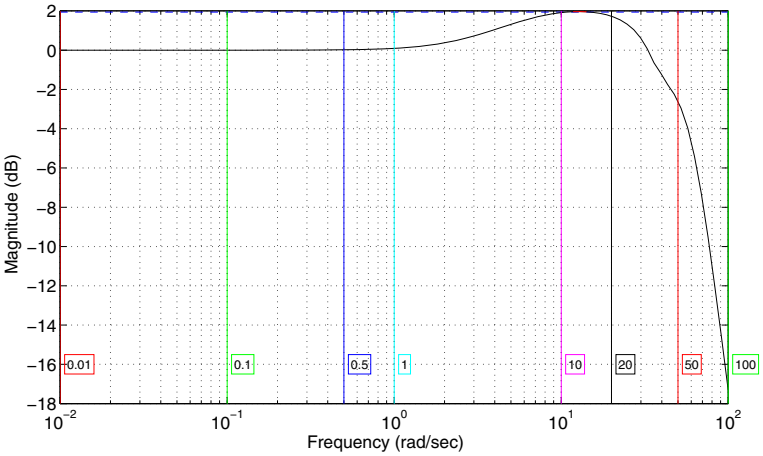

Fig. 20 Analysis of robust stability margin in frequency domain

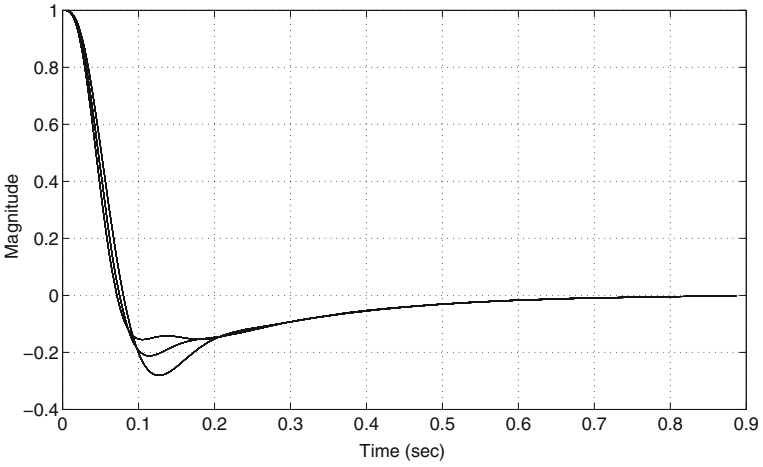

Fig. 21 Analysis of output disturbance rejection time domain step response

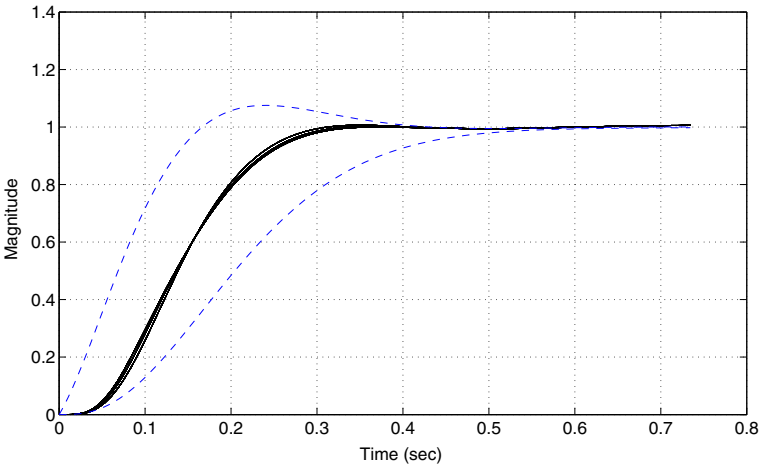

Fig. 22 Analysis of system time domain step response

solid line is under the dashed line, which demonstrates the designed controller and prefilter satisfy the given robust stability specification.

The output disturbance specification is plotted in Fig. 21. In time domain, step signal is utilized as external disturbance to check output disturbance specification. Step signal response decreases to zero at $0.7s$, which can be observed in Fig. 21 and can manifest the designed controller is with the ability to reject the external disturbance.

Figure 22 illustrates the desired reference tracking specifications in frequency domain and demonstrates the closed-loop system transfer function meet all the tracking specifications. In order to intuitively understand the effect of the controller and prefilter, time domain validation is shown in Fig. 22, which can directly indicates

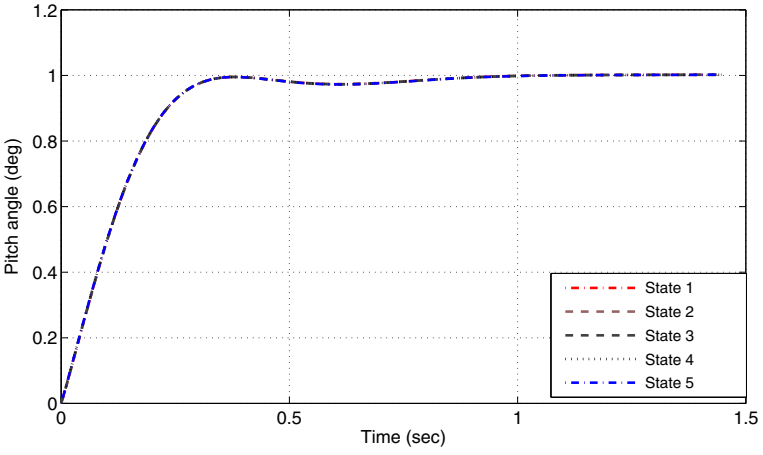

Fig. 23 Step response of nominal pitch system with QFT controller

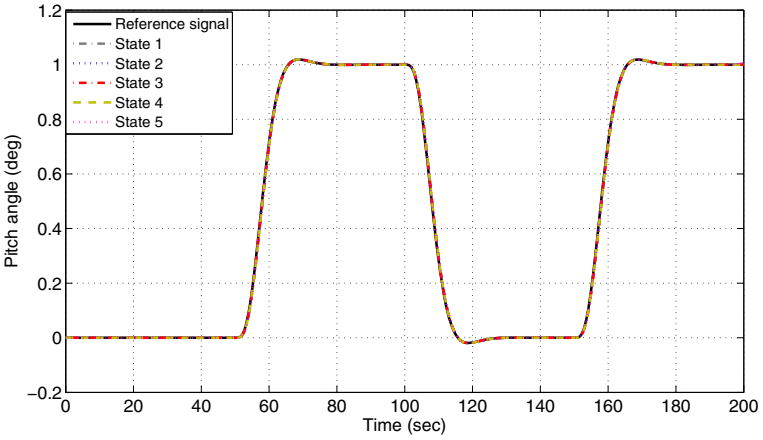

Fig. 24 Tracking response of nominal pitch system with QFT controller

that the step signal of the input can be responded rapidly at $0.3s$ and the tracking specifications are satisfied.

The designed QFT robust controller and prefilter are added to the longitudinal system. Step signal and given reference signal responses of five different states are illustrated in Figs. 23 and 24. States information can be found in Table 1. Significantly, satisfied tracking robust performance of the designed QFT controller is manifested in Figs. 23 and 24.

In order to compare the attitude control performance of the designed robust QFT controller, a LQR controller as illustrated in [35] is synthesized based on the lin-

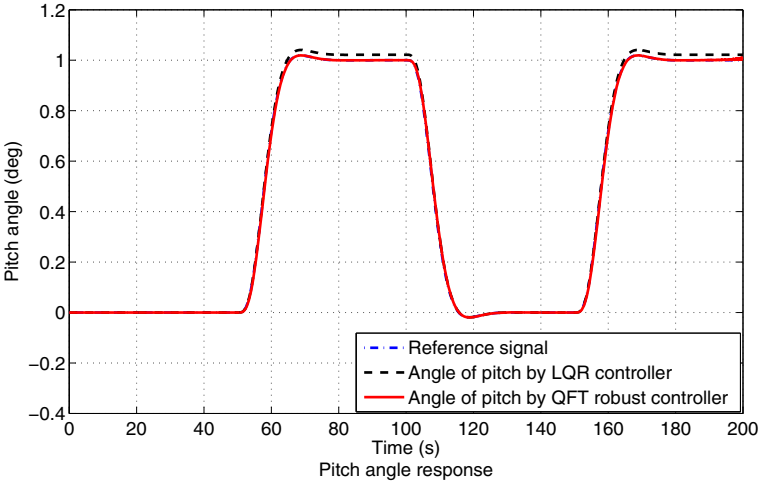

Fig. 25 Tracking response of nominal pitch system with QFT and LQR controller under no uncertainties

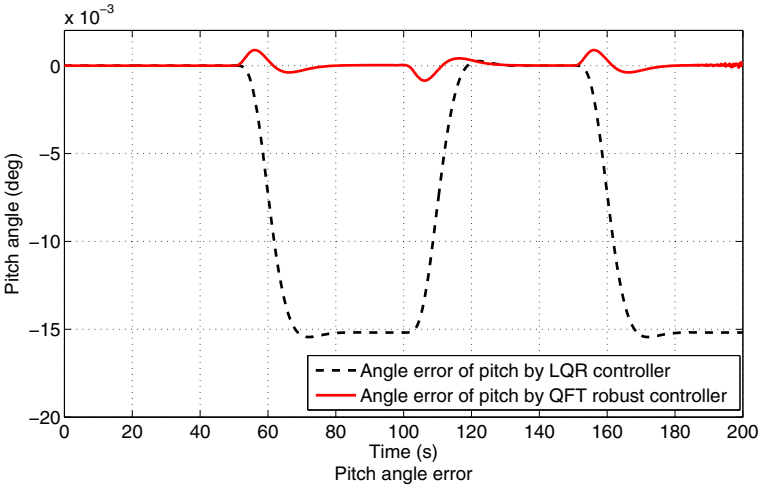

Fig. 26 Tracking response of nominal pitch system with QFT and LQR controller under no uncertainties

earized model. The state space model of the plant is already shown in Eq. 9 and the coefficients can be obtained from Table 1. The weighting matrices Q and R are selected as follows: $Q = \begin{bmatrix} 510 & 0 \\ 0 & 220 \end{bmatrix}$, $R = [0.23]$, and then the control vector K is computed and shown as follows: $K = \begin{bmatrix} -40.9402 & -112.788 \end{bmatrix}$.

As can be seen from Fig. 25, both the QFT and LQR robust controllers can achieve satisfying tracking performance. However, the control input amplitude by the QFT robust controller is more similar to the reference signal baseline than that by the LQR controller, especially the tracking error as depicted in Fig. 26 manifests that the QFT controller can guarantee the plant has better tracking performance.

Conclusions

In this paper, the QFT robust controller and prefilter are designed for dealing with the problem of uncertainty parameter uncertainty, external disturbance and non-minimum phase problem existed in hypersonic aircrafts. The simulation results are presented to demonstrate the effectiveness of the proposed QFT controller and prefilter for hypersonic aircrafts system.

In future, the QFT robust controller design method would be adopted to design the latitudinal model of hypersonic aircrafts which is featured with the characters of multi-input multi-output and strong coupling.

Acknowledgements This work was supported by the National Natural Science Foundation of China under Grants 61873012 and 61503012.

References

1. Wu, L., Yang, X., Li, F.: Nonfragile output tracking control of hypersonic air-breathing vehicles with an LPV model. IEEE/ASME Trans. Mechatron. **18**(4), 1280–1288 (2013)
2. Voland, R.T., Huebner, L.D., McClinton, C.R.: X-43a Hypersonic vehicle technology development. Acta Astronaut. **59**(5), 181–191 (2006)
3. Xu, B., Shi, Z.: Universal Kirging control of hypersonic aircraft model using predictor model without back-stepping. IET Control Theory Appl. **7**(4), 573–583 (2012)
4. Buschek, H., Calise, A.J.: Uncertainty modeling and fixed-order controller design for a hypersonic vehicle model. J. Guid. Control. Dyn. **20**(1), 42–48 (1997)
5. Parker, J.T., Serrani, A., Yurkovich, S., Bolender, M.A., Doman, D.B.: Control-oriented modeling of an air-breathing hypersonic vehicle. J. Guid. Control. Dyn. **30**(3), 856–869 (2007)
6. Liu, H., Li, D., Zuo, Z., Zhong, Y.: Robust three-loop trajectory tracking control for quadrotors with multiple uncertainties. IEEE Trans. Ind. Electron. **63**(4), 2263–2274 (2016)
7. Liu, H., Wang, X., Zhong, Y.: Quaternion-based robust attitude control for uncertain robotic quadrotors. IEEE Trans. Ind. Inf. **11**(2), 406–415 (2015)
8. Liu, H., Zhao, W., Zuo, Z., Zhong, Y.: Robust control for quadrotors with multiple time-varying uncertainties and delays. IEEE Trans. Ind. Electron. **64**(2), 1303–1312 (2017)
9. Xu, H., Mirmirani, M.D., Ioannou, A.: Adaptive sliding mode control design for a hypersonic flight vehicle. J. Guid. Control. Dyn. **27**(5), 829–838 (2004)
10. Fiorentini, L., Serrani, A., Bolender, M.A., Doman, D.B.: Nonlinear robust adaptive control of flexible air-breathing hypersonic vehicles. J. Guid. Control. Dyn. **32**(2), 401–416 (2009)
11. Wilcox, Z.D., MacKunis, W., Bhat, S., Lind, R., Dixion, W.E.: Lyapunov-based exponential tracking control of a hypersonic aircraft with aerothermoelastic effects. J. Guid. Control. Dyn. **33**(4), 1213–1224 (2010)
12. Hu, X., Wu, L., Hu, C., Gao, H.: Fuzzy guaranteed cost tracking control for a flexible air-breathing hypersonic vehicle. IET Control Theory Appl. **6**(9), 1238–1249 (2012)
13. Li, Z., Zhou, W., Liu, H.: Nonlinear robust control of hypersonic aircrafts with interactions between flight dynamics and propulsion systems. ISA Trans. **64**(9), 1–11 (2016)
14. Wang, J., Zong, Q., Tian, B., Liu, H.: Flight control for a flexible air-breathing hypersonic vehicle based on quasi-continuous high-order sliding mode. J. Syst. Eng. Electron. **24**(2), 288–295 (2013)
15. Yang, J., Li, S., Sun, C., Guo, L.: Nonlinear-disturbance-observer-based robust flight control for airbreathing hypersonic vehicles. IEEE Trans. Aerosp. Electron. Syst. **49**(2), 1263–1275 (2013)
16. Hu, X., Hu, C., Wu, L., Gao, H.: Output tracking control for non-minimum phase flexible air-breathing hypersonic vehicle models. J. Aerosp. Eng. **28**(2), 1–11 (2015)
17. Fiorentini, L., Serrani, A.: Adaptive restricted trajectory tracking for a non-minimum phase hypersonic vehicle model. Automatica **48**(7), 1248–1261 (2012)
18. Hovakimyana, N., Vitae, A., Yangb, B., Vitae, A., Calise, A.J.: Adaptive output feedback control methodology applicable to non-minimum phase nonlinear systems. Automatica **42**(4), 513–522 (2006)
19. Horowitz, I., Sidi, M.: Synthesis of feedback systems with large plant ignorance for prescribed time domain tolerance. Int. J. Control. **16**(2), 287–309 (1972)
20. Horowitz, I., Sidi, M.: Synthesis of feedback systems with nonlinear time uncertain plants to satisfy quantitative performance specifications. IEEE Trans. Autom. Control **64**(3), 123–130 (1976)
21. Horowitz, I.: Quantitative synthesis of uncertain multiple input-multiple output feedback systems. Int. J. Control. **30**(1), 81–106 (1979)
22. Kerr, M., Jayasuriya, S., Asokanthan, S.: Robust stability of sequential MIMO QFT designs. ASME Journal of Dynamic Systems, Measurement and Control **127**(2), 250–256 (2005)
23. Kerr, M., Jayasuriya, S., Asokanthan, S.: On stability in non-sequential MIMO QFT designs. ASME Journal of Dynamic Systems, Measurement and Control **127**(1), 98–104 (2005)
24. Boje, E.: Non-diagonal controllers in MIMO quantitative feedback design. Int. J. Robust Nonlinear Control **12**(4), 303–320 (2002)
25. Horowitz, I., Sidi, M.: Optimum synthesis of non-minimum phase feedback system with plant uncertainty. Int. J. Control. **27**(3), 361–386 (1978)
26. Chen, W., Ballance, D.: QFT Design for uncertain non-minimum phase and unstable plants revisited. Int. J. Control. **74**(9), 957–965 (2001)

27. Reynolds, R., Pachter, M., Hoipis, C.H.: Full envelop flight control system design using quantitative feedback theory. J. Guid. Control. Dyn. **19**(1), 23–29 (1996)
28. Janardanan, J., Jayakumar, M.: Robust longitudinal flight controller design for a hypersonic re-entry vehicle. In: 14Th AIAA/AHI Space Planes and Hypersonic Systems and Technologies Conference, Canberra, Australia, pp. 1–7 (2006)
29. Nataraj, P.S.V.: Computation of QFT bounds for robust tracking specifications. Automatica **38**(2), 327–334 (2002)
30. Chait, Y., Yaniv, O.: Multi-input/single-output computer-aided control design using the quantitative feedback theory. Int. J. Robust Nonlinear Control **3**(23), 47–54 (1993)
31. Zhao, Y., Jayasuriya, S.: On the generation of QFT bounds for general interval plants. ASME Journal of Dynamic Systems Measurement and Control **116**(12), 618–627 (1994)
32. Rodrigues, J., Chait, Y., Yaniv, O.: An efficient algorithm for computing QFT bounds. ASME Journal of Dynamic Systems Measurement and Control **119**(11), 548–552 (1997)
33. Nataraj, P.: Interval QFT: a mathematical and computational enhancement of QFT. Int. J. Robust Nonlinear Control **12**(4), 385–402 (2002)
34. Yu, G., Li, H.: Hierarchical structured robust adaptive attitude controller design for reusable launch vehicles. J. Syst. Eng. Electron. **26**(4), 813–825 (2015)
35. Liu, H., Lu, G., Zhong, Y., Robust, L.Q.R.: Attitude control of a 3-DOF laboratory helicopter for aggressive maneuvers. IEEE Trans. Ind. Electron. **60**(10), 4627–4636 (2013)